How to cite: *Angew. Chem. Int. Ed.* **2021**, *60*, 290–296
International Edition: doi.org/10.1002/anie.202008178
German Edition: doi.org/10.1002/ange.202008178

Electrochemistry

Hydrogen Bonding Enhances the Electrochemical Hydrogenation of Benzaldehyde in the Aqueous Phase

Udishnu Sanyal, Simuck F. Yuk, Katherine Koh, Mal-Soon Lee, Kelsey Stoerzinger, Difan Zhang, Laura C. Meyer, Juan A. Lopez-Ruiz, Abhi Karkamkar, Jamie D. Holladay, Donald M. Camaioni, Manh-Thuong Nguyen, Vassiliki-Alexandra Glezakou, Roger Rousseau, Oliver Y. Gutiérrez,* and Johannes A. Lercher**

Abstract: *The hydrogenation of benzaldehyde to benzyl alcohol on carbon-supported metals in water, enabled by an external potential, is markedly promoted by polarization of the functional groups. The presence of polar co-adsorbates, such as substituted phenols, enhances the hydrogenation rate of the aldehyde by two effects, that is, polarizing the carbonyl group and increasing the probability of forming a transition state for H addition. These two effects enable a hydrogenation route, in which phenol acts as a conduit for proton addition, with a higher rate than the direct proton transfer from hydronium ions. The fast hydrogenation enabled by the presence of phenol and applied potential overcompensates for the decrease in coverage of benzaldehyde caused by competitive adsorption. A higher acid strength of the co-adsorbate increases the intensity of interactions and the rates of selective carbonyl reduction.*

Introduction

Electrochemical hydrogenation (ECH) of organic compounds has the potential to enable the use of aqueous phase carbon waste feedstocks as the basis for decentralized synthesis of fuel components and chemicals.[1,2] Thus, understanding the mechanism of ECH has become a critical necessity.[3,4] Most organic compounds diluted in aqueous feedstocks are functionalized arenes (e.g., phenol derivatives), alcohols, aldehydes, ketones, and carboxylic acids. A large variety of these unsaturated groups can be reduced via ECH, including aromatic rings in phenolic compounds,[2,5–8] carbonyl groups in aldehydes, ketones and sugars,[9–11,12,13–15] and C=C double bonds.[16–19] However, the complexity of the chemistry at the cathode leads to challenging conditions for understanding and controlling these reactions at the molecular level.

Evidence exists that hydrogenation of phenol (a model compound for functionalized arenes) on Pt group metals follows a mechanism, in which the organic compound adsorbs molecularly and reacts with adsorbed hydrogen atoms.[8,20,21] The elementary steps are independent whether the hydrogen atoms are electrochemically generated by reduction of hydronium ions or by dissociation of H_2. Electrocatalytic hydrogenation of carbonyl groups may, however, also involve proton and electron transfer in the rate determining step (i.e., proton coupled electron transfer [PCET]).[10,15]

Regardless of the specifics of the hydrogen addition step, molecules such as phenol and benzaldehyde are adsorbed prior to hydrogenation; that is, hydrogenation occurs via an inner-sphere hydrogen addition or electron transfer mechanism.[7,23–25] This leads to competition for adsorption sites, if several reacting species are present. Thus, it is to be expected that conversion rates of a particular substrate decrease, when other reactive substrates are present simultaneously.[26,27–29] We report here, however, the synergistic interactions of co-adsorbed reactive molecules that activate the targeted functional group and enhance the rate constant of selective hydrogenation.

Results and Discussion

Impact of (substituted) Phenols on Electrocatalytic Reduction

The ECH of benzaldehyde to benzyl alcohol is catalyzed by Pd/C at a cathode potential of −0.1 V vs. a reversible hydrogen electrode (RHE). The rates increased more than twofold in the presence of phenol when its concentrations

[*] Dr. U. Sanyal, Dr. S. F. Yuk, Dr. K. Koh, Dr. M.-S. Lee, Dr. K. Stoerzinger, Dr. D. Zhang, L. C. Meyer, Dr. J. A. Lopez-Ruiz, Dr. A. Karkamkar, Dr. J. D. Holladay, Dr. D. M. Camaioni, Dr. M.-T. Nguyen, Dr. V.-A. Glezakou, Dr. R. Rousseau, Dr. O. Y. Gutiérrez, Prof. J. A. Lercher
Institute for Integrated Catalysis, Pacific Northwest National Laboratory
P.O. Box 999, Richland, WA 99352 (USA)
E-mail: roger.rousseau@pnnl.gov
oliver.gutierrez@pnnl.gov
Dr. K. Stoerzinger
School of Chemical, Biological and Environmental Engineering, Oregon State University
Corvallis, OR 97331 (USA)
Prof. J. A. Lercher
Department of Chemistry and Catalysis Research Center Institution, TU München
Lichtenbergstrasse 4, 85747 Garching (Germany)
E-mail: johannes.lercher@ch.tum.de
Supporting information and the ORCID identification number(s) for the author(s) of this article can be found under: https://doi.org/10.1002/anie.202008178.

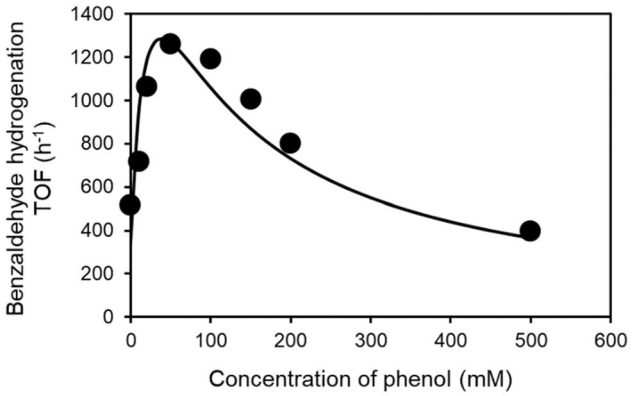

Figure 1. Turnover frequencies (TOFs) of electrocatalytic hydrogenation of benzaldehyde on Pd/C in the presence of varying concentrations of phenol. Reaction conditions: sodium acetate-acetic acid buffer electrolyte (3 M, pH 5.2), 20 mM benzaldehyde, room temperature, 1 bar N_2 flow, −0.1 V vs. RHE. The corresponding data points were fitted with a co-adsorption model as described in the supporting information.

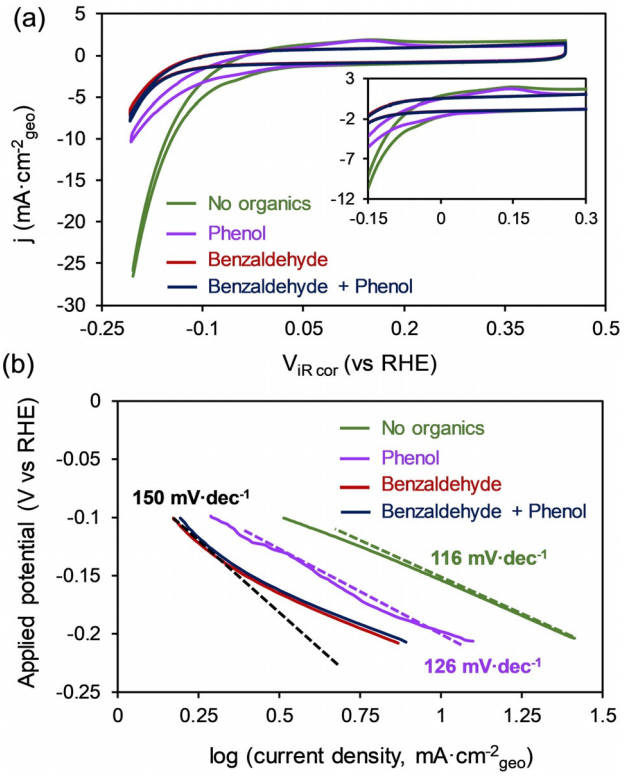

Figure 2. a) Cyclic voltammograms measured with Pd/C in the presence of benzaldehyde, phenol and an equimolar mixture of phenol and benzaldehyde (inset shows the region of onset potential). b) Tafel slopes measured in the presence and absence of organics. Reaction conditions: Sodium acetate-acetic acid (3 M) buffer (pH 5.2) electrolyte, room temperature, 20 mM organic compounds, 1 bar N_2 flow.

increased up to ≈50 mM (Figure 1). Benzaldehyde ECH rates declined with more phenol present but were still higher with 200 mM phenol than with the parent solution containing only benzaldehyde (801 h^{-1} and 517 h^{-1}, respectively). At high phenol concentration (500 mM), the rate of benzaldehyde hydrogenation, normalized to exposed Pd (turnover frequency [TOF]) decreased to 396 h^{-1}. The TOF of H_2 evolution (HER), the prevalent reaction competing with benzaldehyde hydrogenation, also increased from 26 h^{-1} in the presence of solely benzaldehyde to ≈40 h^{-1} in the presence of 20–100 mM phenol. The HER TOF increased to 133 h^{-1} and 469 h^{-1} with 200 mM and 500 mM phenol, respectively (see Figure S1 in the Supporting Information). The HER TOF in the presence of only phenol (20 mM) was 1881 h^{-1}. In the absence of organic compounds under otherwise identical conditions, the HER TOF was 2647 h^{-1} (i.e., an order of magnitude higher than in the presence of benzaldehyde).

Cyclic voltammograms (CV) in pure electrolyte (Figure 2a) showed a shoulder at −0.04 V vs. RHE in the cathodic scan, which is attributed to the formation of Pd hydride overlapping with the HER current.[30,31] The peak of the corresponding reverse process, that is, the oxidation of hydride to hydrogen and Pd metal was observed at 0.15 V vs. RHE.

The addition of 20 mM phenol decreased, but did not fully suppress, hydride formation and oxidation currents. The addition of further benzaldehyde, in contrast, reduced hydride formation completely and shifted the current onset to negative potentials by ≈0.1 V. The CV curve was identical, if only 20 mM benzaldehyde was present. We conclude that the presence of phenol and benzaldehyde adsorbing on Pd, decreased the concentration of accessible Pd available to transfer electrons to H^+. This is in perfect agreement with the effect of the presence of organic compounds on the underpotential generation of adsorbed H on Pt.[32–34]

The Tafel slope for HER was 116 mV dec^{-1} in pure electrolyte at pH 5.2 (Figure 2b), which indicates that the first electron transfer step to the hydronium ion (i.e., the Volmer step) is rate-determining under the experimental conditions.[35] The Tafel slope changed to 126 mV dec^{-1} in the presence of phenol and to ≈150 mV dec^{-1} in the presence of benzaldehyde and absence of added phenol. Hence, phenol has little influence on the electron transfer, while the influence of benzaldehyde is notable.

To probe this different behavior, we use electrochemical impedance spectroscopy (EIS). In the Nyquist plots (Figure S2), the diameter of the main semicircle is attributed to the charge transfer resistance, which is inversely proportional to the rate of the Volmer step.[36,37] In the presence of benzaldehyde or phenol, the diameter of the main semicircles (i.e., the charge transfer resistance) markedly increased. The diameter was larger with benzaldehyde than with phenol at identical other concentrations. This indicates that the sorption of both aromatic compounds decreases the rates of hydronium ion reduction or changes the nature of the charge transfer process.

Mechanism of Carbonyl Hydrogenation in the Presence of Phenol

The stronger impact of benzaldehyde than of phenol on the Tafel slope for HER and on the EIS spectra suggest that the electron transfer processes change, if benzaldehyde is

present (in contrast to phenol, which only seems to decrease the availability of sites for electron transfer). Thus, we hypothesize that in the presence of benzaldehyde, hydronium-ion reduction is replaced by proton addition followed by or coupled with electron addition, implying that hydrogenation proceeds through a PCET mechanism. This claim is supported by the higher rates of ECH observed in presence of higher concentrations of acid groups on the carbon support (but not on H_2 evolution or on thermocatalytic hydrogenation). Additionally, theoretical calculations have indicated that the reduction of aldehydes in the presence of cathodic potentials tends to follow a PCET mechanism.[10,38–40] The fact that phenol enhances solely benzaldehyde ECH (Figure 1), suggests that hydrogenation proceeds in presence and absence of an external electric potential via different pathways, via a PCET mechanism in the first case and by sequential hydrogen addition in the latter.

We probed the energetics of this reaction step by DFT-based *ab-initio* molecular dynamic simulations with and without the presence of co-adsorbed phenol on a Pd(111) surface (see Figures S6 and S7). It is important to note that Pd tends to form β-hydride upon the application of negative potentials. However, this phase transition is suppressed in the presence of benzaldehyde as shown by the CV experiments (Figure 2a) and our recent in situ X-ray absorption near edge structure study.[41] Hence, β-hydride was not considered in the present calculations.

The most stable structure of adsorbed benzaldehyde resulting from these calculations is one parallel to the surface (Figure S3a), while the co-adsorbed phenol is tilted away from the surface as shown in Figure S3b. This finding is in agreement with the findings of previous studies.[42–45] The carbonyl group of co-adsorbed benzaldehyde interacts directly with the hydroxyl group of phenol (see Figure S3b). CMD simulations further corroborate a favorable benzaldehyde interaction with phenol rather than with another benzaldehyde molecule, as indicated by their radial distribution profiles (Figure S4).

Figure 3 follows the enthalpic changes along the hydrogenation cycle of benzaldehyde by a PCET mechanism, with and without the co-adsorbed phenol on Pd(111). The explored routes of possible hydrogenation mechanisms are summarized in Figures S6 and S7 (along with the detailed analysis on relative enthalpy of reaction intermediates). In the absence of phenol, the energy needed to bring a hydronium ion to a position adjacent to benzaldehyde is approximately 89 kJ mol^{-1} (see Figure 3, upper cycle). As hydrogenation proceeds, the energy decreases first slightly and then sharply (from state **2a** to **3a** and **4a** in Figure 3). In contrast, when phenol is present at the surface, the energy penalty to bring a hydronium ion next to benzaldehyde is decreased to ≈15 kJ mol^{-1} (see Figure 3, from state **2b** to **3b**). The energy landscape to the hydrogenated product is flatter (from state **3b** to **4b** and **5b**) than in the absence of phenol because phenol stabilizes all intermediate steps to similar extents (Route 4 in Figure S7).

We note that benzaldehyde is more stable than benzyl alcohol in the presence and the absence of phenol (by 7 kJ mol^{-1} and 14 kJ mol^{-1}, respectively). However, phenol

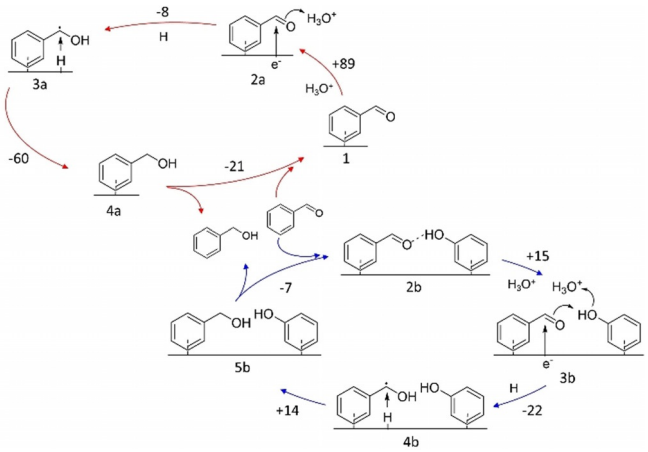

Figure 3. DFT-derived enthalpic changes in the hydrogenation of benzaldehyde by proton-coupled electron transfer, with and without the presence of co-adsorbed phenol on Pd(111). The numbers below the structures are the labels of the steps that they represent (these labels coincide with those used in Figures S6 and S7). The numbers next to the arrows represent enthalpic differences between two states with and without phenol (blue and red cycle, respectively) in kJ mol^{-1}. Calculations were performed on a charged surface with ≈0.01 e$^-$/surface Pd atom.

stabilizes the states in between. Thus, the second hydrogenation, alone, is slightly endothermic in the presence of phenol but exothermic (14 kJ mol^{-1} and −60 kJ mol^{-1}, respectively) in its absence.

In the route in the presence of phenol, H_3O^+ delivers a proton to phenol, which in turn, transfers its proton to neighboring benzaldehyde. Thus, we postulate that one of the roles of phenol is to act as a conduit for proton transfer, which enhances hydrogenation of benzaldehyde.

To probe the feasibility of this proposal, we analyzed the Bader charges of adsorbed phenol and benzaldehyde. The OH group of phenol becomes negatively charged upon adsorption, thus acting as stronger nucleophile. In turn, the carbonyl group of benzaldehyde also becomes polarized, rendering it more susceptible to proton transfer (see Table S2 and Figure S8 along with the detailed analysis on Bader charges of adsorbed molecules).

The DFT calculations also indicate that transferring a proton from the hydronium ion (with accompanying charge transfer from the metal surface) to the basic carbonyl oxygen via phenol is thermodynamically favored over transferring the H atom from the Pd surface by ≈40 kJ mol^{-1} (Route 4 and Route 2 in Figure S7). Thus, we conclude that co-adsorbed phenol acts as a conduit for protons from bulk water, but not as a source of the proton itself. This is consistent with the much lower pK_a of hydronium ion compared to phenol (i.e., pK_a = −1.74 and 10, respectively).

The pathway in which the hydronium ion acts as proton donor (without involvement of phenol) passes higher energies than this indirect path (see Figure S7). Such a role of phenol as a proton relay is equivalent to the role of the extended coordination environment in molecular electrocatalysis.[46] This theoretical analysis provides a qualitative rationale for the co-adsorption effect. However, we have not directly

computed transition energy barriers. Thus, we cannot definitively account for experimental rates that are much slower than the large energy differences suggest. Moreover, the experimental kinetics of electron transfer may be retarded by an unfavorable charge transfer coefficient (unknown for our reaction) and by the reversible potential at the surface, which is expected to change as the local concentration of hydronium ions increases due to the presence on phenol.

Therefore, this enhancement in benzaldehyde hydrogenation rate in the presence of phenol is postulated to originate from: 1) polarization and, hence, activation of the carbonyl group through interactions with the hydroxy group of phenol and 2) increasing the local availability of hydronium ions for proton transfer to benzaldehyde. Such a hydrogen bonded benzaldehyde-phenol complex has been proposed to promote PCET processeses.[47] Complex molecular interactions in water that result in bond polarization and enhanced rates have been recently summarized in Ref. [48]. Scheme 1 illustrates the central mechanistic proposal, that is, both phenol and benzaldehyde co-adsorb on the surface, and the carbonyl in benzaldehyde reacts easier with a hydronium ion, when it is polarized by a hydrogen bond with phenol. This protonation is coupled with a one-electron transfer from the metal to complete the first hydrogenation step. A second (direct) hydrogen addition to the first intermediate produces the final benzyl alcohol product.

Thus, we conclude that 1) aromatic compounds adsorb competitively on Pd; 2) co-adsorbed phenol and benzaldehyde interact; 3) electron transfers are involved in the rate determining steps in HER and ECH, and 4) the rate constant of ECH and the adsorption constant of the reacting substrates are a function of the electrochemical potential. Consequently, the rates of HER (r_{HER}) and electrocatalytic hydrogenation (r_{ECH}) can be described by Equations (1) and (2), in which k_{HER} and k_{ECH} are potential-dependent rate constants; $a_{H_3O^+}$ is the activity of hydronium ions; θ_{RCHO}, is the surface coverage of benzaldehyde; and θ_V is the concentration of free adsorption sites.

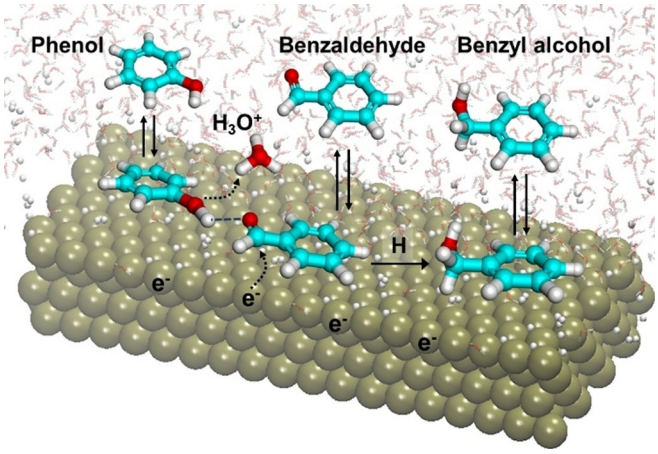

Scheme 1. Schematic diagram of the electrocatalytic hydrogenation of the H-bonded complex formed upon adsorption of benzaldehyde and phenol. The double arrows denote adsorption and the dashed arrows illustrate the flow of electrons accompanying the deprotonation of the hydronium ion and the reduction of the carbonyl group.

$$r_{HER} = k_{HER}\theta_V\, a_{H_3O^+} \quad (1)$$

$$r_{ECH} = k_{ECH}\theta_{RCHO}\, a_{H_3O^+} \quad (2)$$

Equation (2) does not reflect the rate enhancement for benzaldehyde ECH in presence of phenol. This rate increase is concluded to be related to a new reaction pathway with both a surface coverage and a rate constant different from those outlined in Equation (2). We surmise that the two pathways are additive and that the concentration of H-bonding complexes is a function of the coverages of benzaldehyde and phenol. This is expressed in Equation (3), in which θ_{ROH}, is the surface coverage of phenol, k'_{ECH} is the rate constant for the hydrogenation of the H-bonded complex and $K_{[RCHO\text{-}ROH]}$ is the equilibrium constant of the complex formation.

$$r = k_{ECH}\theta_{RCHO}\, a_{H_3O^+} + k'_{ECH}\, K_{[RCHO\text{-}ROH]}\, \theta_{RCHO}\, \theta_{ROH}\, a_{H_3O^+} \quad (3)$$

The rate expression reflects the dependence on the product of the two coverages that appears to reach a maximum at around 50 mM of phenol (Figure 1, for details see the SI). Using CV, the standard free energies of adsorption of benzaldehyde and phenol on the Pd/C catalyst were determined.[34] Together with the ECH rates, we used them to fit the kinetic model of Equation (3) as described in the supporting information. The results confirmed the hypothesis that the maximum rate enhancement is achieved at equivalent coverages of benzaldehyde and phenol. The average rate constant for this pathway, k'_{ECH}, was three times higher than k_{ECH}.

As the polarization of the carbonyl group of benzaldehyde is critical for the rate, changing the acid strength of the co-adsorbed phenol should influence the rate enhancement. Indeed, as shown in Figure 4 (and Figure S11) the rate of benzaldehyde ECH increased linearly with the pK_a of the co-adsorbed molecule.[49,50] This indicates that the strength of the electron pair donor- acceptor interactions leading to the polarization of the C=O bond and the proton shuttling abilities (i.e., the stabilization of the transition state, in which the proton is transferred to benzaldehyde via phenol) are enhanced by a higher acid strength.

Under open circuit voltage conditions, with 1 bar H_2, the rate of benzaldehyde hydrogenation was independent of the phenol concentration (Figure S10). This clearly indicates that hydrogenation with equilibrated adsorption of H_2 is fundamentally different to ECH. Hydrogenation with H_2 follows a Langmuir-Hinshelwood mechanism, in which adsorbed H forms upon H_2 dissociation and reacts with adsorbed benzaldehyde.[14] Thus, the constant rate of benzaldehyde hydrogenation in the presence of phenol indicates that the hydrogen coverage compensates the decreasing surface coverage of benzaldehyde as phenol concentration increases. This proposal is in line with the better ability of benzaldehyde to displace hydrogen from the metal surface than phenol.[34]

Hydrogenation of Benzaldehyde on Different Metals

We also observed the rate enhancement of benzaldehyde ECH by phenol with other metals. The rates increased in the

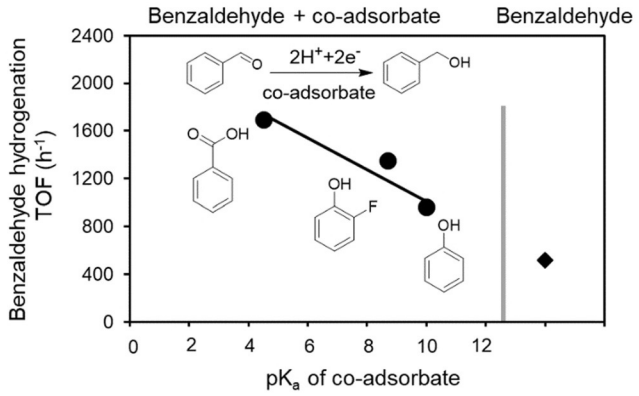

Figure 4. TOFs of benzaldehyde hydrogenation in the presence of different co-adsorbed organics on Pd/C. The rate of benzaldehyde hydrogenation in the absence of co-adsorbate is shown in the most-right point (◆). Reaction conditions: sodium acetate-acetic acid (3 M) buffer (pH 5.2) electrolyte, 20 mM benzaldehyde, 20 mM co-adsorbate, room temperature, 1 bar N_2 flow, −0.1 V vs. RHE.

order Rh/C < Ru/C < Pd/C < Cu/C (Figure 5, Figure S12, S13 and Table S3). This trend is inversely proportional to the binding energies (E_b) of benzaldehyde on charged metal surfaces as determined computationally: −0.7 eV (Cu) < −3.2 eV (Pd) < −4.8 eV (Ru) < −5.4 eV (Rh).[51] Thus, the rate enhancement observed by phenol co-adsorption is hypothesized to be related to the ability of phenol to adsorb at the metal surface displacing benzaldehyde. This is also reflected in the changes of reaction order in benzaldehyde ranging from ≈0 in the absence of phenol to >0 in the presence of phenol (Figure S14 and Figure S15).

Surprisingly, HER rates also increased in the presence of phenol, despite the parallel hydrogenation of the organic substrate. At present, we hypothesize that the higher rates are enabled by the increase of the concentration of hydronium ion induced by the sorption of molecules with polar groups or to lower kinetic barriers for their reduction through shuttling mechanisms similar to the mechanism leading to the enhancement of ECH rates. The positive impact of phenol on HER rates is attributed to the increasing concentration of hydronium ions at the interface, which has been identified to cause the positive impact of proton carriers on HER rates on gold electrodes.[52] The different degrees to which phenol affects HER for different metals is in turn attributed to the differences between the binding energies of organic compounds and hydrogen.[53–55]

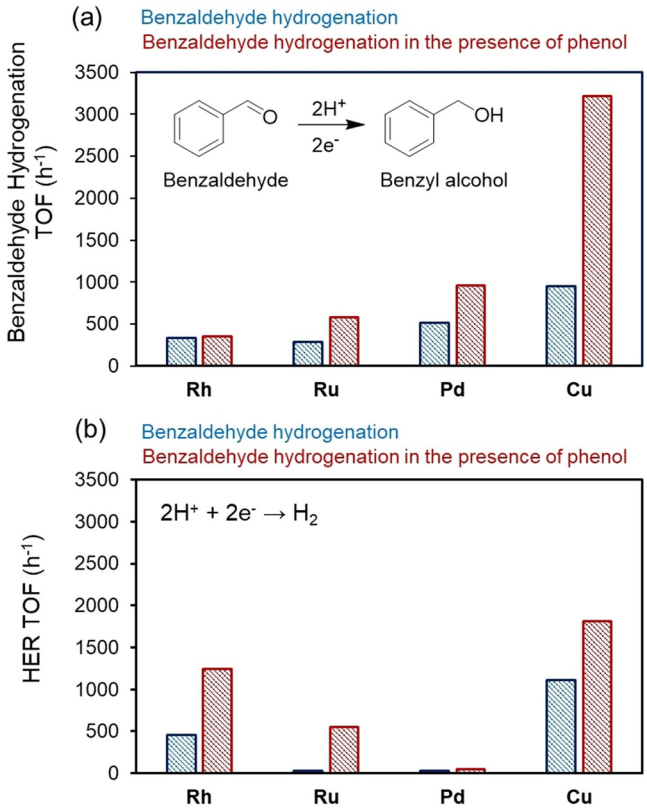

Figure 5. TOFs of a) benzaldehyde hydrogenation and the associated b) HER reaction in the absence and the presence of phenol on Rh/C, Ru/C, Pd/C and Cu/C. Reaction conditions: sodium acetate-acetic acid (3 M) buffer (pH 5.2) electrolyte, 20 mM benzaldehyde and 20 mM phenol, room temperature, 1 bar N_2 flow, −0.1 V vs. RHE for Rh/C, Ru/C, Pd/C and −0.5 V vs. RHE for Cu/C.

Conclusion

Results of the present study show that in the presence of an applied electrical potential, intermolecular interactions among adsorbed benzaldehyde and adsorbed polar aromatic compounds enhance the rate constants of electrochemical hydrogenation of carbonyl groups in aldehydes such as benzaldehyde. We attribute this enhancement to 1) the polarization of the carbonyl group in benzaldehyde by hydrogen bonding interactions with phenol and 2) a more facile proton-coupled electron transfer pathway enabled by a transition state stabilized by phenol.

As a result, the co-adsorbate enables a hydrogenation route for the carbonyl group with lower activation energy than in the absence of phenolic compounds and increases the concentration of available hydronium ions. We speculate that the latter effect also enhances the rates of H_2 evolution. The higher rate constant of co-adsorbate-mediated hydrogenation route overcompensates the decreasing coverage of benzaldehyde. The rate is highest if both reaction partners are present in equimolar concentrations at the surface. For different metals, the rate enhancement is positively correlated with the adsorption strength of benzaldehyde (i.e., with the ability of phenol to partly displace it).

These findings demonstrate the ability to enhance electrocatalytic rates of hydrogenation by subtly adjusting the composition of the organic solvents and opens new pathways to control selective transformations.

Acknowledgements

The research described in this paper is part of the Chemical Transformation Initiative at Pacific Northwest National Laboratory (PNNL), conducted under PNNL's Laboratory

Directed Research and Development Program. D.M.C. and J.A.L. were supported by the U.S. Department of Energy (DOE), Office of Science, Office of Basic Energy Sciences, Division of Chemical Sciences, Geosciences and Biosciences (Transdisciplinary Approaches to Realize Novel Catalytic Pathways to Energy Carriers, FWP 47319). Computational resources were provided by PNNL's Research Computing facility and the National Energy Research Scientific Computing Center (NERSC), which is a DOE Office of Science User Facility. Open access funding enabled and organized by Projekt DEAL.

Conflict of interest

The authors declare no conflict of interest.

Keywords: electrochemistry · electron transfer · hydrogen bonding · reduction · supported catalysts

[1] T. E. Lister, L. A. Diaz, M. A. Lilga, A. B. Padmaperuma, Y. Lin, V. M. Palakkal, C. G. Arges, *Energy Fuels* **2018**, *32*, 5944 – 5950.
[2] C. H. Lam, C. B. Lowe, Z. Li, K. N. Longe, J. T. Rayburn, M. A. Caldwell, C. E. Houdek, J. B. Maguire, C. M. Saffron, D. J. Miller, J. E. Jackson, *Green Chem.* **2015**, *17*, 601 – 609.
[3] B. A. Frontana-Uribe, R. D. Little, J. G. Ibanez, A. Palma, R. Vasquez-Medrano, *Green Chem.* **2010**, *12*, 2099 – 2119.
[4] E. J. Horn, B. R. Rosen, P. S. Baran, *ACS Cent. Sci.* **2016**, *2*, 302 – 308.
[5] K. J. Carroll, T. Burger, L. Langenegger, S. Chavez, S. T. Hunt, Y. Román-Leshkov, F. R. Brushett, *ChemSusChem* **2016**, *9*, 1904 – 1910.
[6] Z. Li, M. Garedew, C. H. Lam, J. E. Jackson, D. J. Miller, C. M. Saffron, *Green Chem.* **2012**, *14, 0*.
[7] Y. Song, S. H. Chia, U. Sanyal, O. Y. Gutierrez, J. A. Lercher, *J. Catal.* **2016**, *344*, 263 – 272.
[8] Y. Song, O. Y. Gutiérrez, J. Herranz, J. A. Lercher, *Appl. Catal. B* **2016**, *182*, 236 – 246.
[9] Y. Kwon, K. J. P. Schouten, J. C. van der Waal, E. de Jong, M. T. M. Koper, *ACS Catal.* **2016**, *6*, 6704 – 6717.
[10] C. J. Bondue, M. T. M. Koper, *J. Catal.* **2019**, *369*, 302 – 311.
[11] X. H. Chadderdon, D. J. Chadderdon, J. E. Matthiesen, Y. Qiu, J. M. Carraher, J.-P. Tessonnier, W. Li, *J. Am. Chem. Soc.* **2017**, *139*, 14120 – 14128.
[12] Y. Kwon, M. T. Koper, *ChemSusChem* **2013**, *6*, 455 – 462.
[13] U. Sanyal, J. A. Lopez-Ruiz, A. Padmaperuma, J. Holladay, O. Y. Gutiérrez, *Org. Process Res. Dev.* **2018**, *22*, 1590 – 1598.
[14] Y. Song, U. Sanyal, D. Pangotra, J. D. Holladay, D. M. Camaioni, O. Y. Gutiérrez, J. A. Lercher, *J. Catal.* **2018**, *359*, 68 – 75.
[15] J. A. Lopez-Ruiz, U. Sanyal, J. Egbert, O. Y. Gutiérrez, J. Holladay, *ACS Sustainable Chem. Eng.* **2018**, *6*, 16073 – 16085.
[16] J. E. Matthiesen, J. M. Carraher, M. Vasiliu, D. A. Dixon, J.-P. Tessonnier, *ACS Sustainable Chem. Eng.* **2016**, *4*, 3575 – 3585.
[17] J. E. Matthiesen, M. Suástegui, Y. Wu, M. Viswanathan, Y. Qu, M. Cao, N. Rodriguez-Quiroz, A. Okerlund, G. Kraus, D. R. Raman, Z. Shao, J.-P. Tessonnier, *ACS Sustainable Chem. Eng.* **2016**, *4*, 7098 – 7109.
[18] L. Xin, Z. Zhang, J. Qi, D. J. Chadderdon, Y. Qiu, K. M. Warsko, W. Li, *ChemSusChem* **2013**, *6*, 674 – 686.
[19] Y. Qiu, L. Xin, D. J. Chadderdon, J. Qi, C. Liang, W. Li, *Green Chem.* **2014**, *16*, 1305 – 1315.
[20] U. Sanyal, J. Lopez-Ruiz, A. B. Padmaperuma, J. Holladay, O. Y. Gutiérrez, *Org. Process Res. Dev.* **2018**, *22*, 1590 – 1598.
[21] U. Sanyal, Y. Song, N. Singh, J. L. Fulton, J. Herranz, A. Jentys, O. Y. Gutiérrez, J. A. Lercher, *ChemCatChem* **2019**, *11*, 575 – 582.
[22] a) J. Shangguan, Y.-H. C. Chin, *ACS Catal.* **2019**, *9*, 1763 – 1778; b) Z. Zhao, R. Bababrik, W. Xue, Y. Li, N. M. Briggs, D.-T. Nguyen, U. Nguyen, S. P. Crossley, S. Wang, B. Wang, D. E. Resasco, *Nat. Catal.* **2019**, *2*, 431 – 436.
[23] C. Zhao, J. He, A. A. Lemonidou, X. Li, J. A. Lercher, *J. Catal.* **2011**, *280*, 8 – 16.
[24] J. He, C. Zhao, J. A. Lercher, *J. Am. Chem. Soc.* **2012**, *134*, 20768 – 20775.
[25] M. Wang, H. Shi, D. M. Camaioni, J. A. Lercher, *Angew. Chem. Int. Ed.* **2017**, *56*, 2110 – 2114; *Angew. Chem.* **2017**, *129*, 2142 – 2146.
[26] Y. Chen, D. J. Miller, J. E. Jackson, *Ind. Eng. Chem. Res.* **2007**, *46*, 3334 – 3340.
[27] C. P. Rader, H. A. Smith, *J. Am. Chem. Soc.* **1962**, *84*, 1443 – 1449.
[28] M. S. Lylykangas, P. A. Rautanen, A. O. I. Krause, *Ind. Eng. Chem. Res.* **2002**, *41*, 5632 – 5639.
[29] V. Růžička, L. Červený, *Catal. Rev.* **1982**, *24*, 503 – 566.
[30] L. D. Burke, J. K. Casey, *J. Electrochem. Soc.* **1993**, *140*, 1292 – 1298.
[31] A. Zalineeva, S. Baranton, C. Coutanceau, G. Jerkiewicz, *Sci. Adv.* **2017**, *3*, e1600542.
[32] K. Sasaki, A. Kunai, J. Harada, S. Nakabori, *Electrochim. Acta* **1983**, *28*, 671 – 674.
[33] M. D. Obradović, J. Lessard, G. Jerkiewicz, *J. Electroanal. Chem.* **2010**, *649*, 248 – 256.
[34] N. Singh, U. Sanyal, J. L. Fulton, O. Y. Gutiérrez, J. A. Lercher, C. T. Campbell, *ACS Catal.* **2019**, *9*, 6869 – 6881.
[35] T. Shinagawa, A. T. Garcia-Esparza, K. Takanabe, *Sci. Rep.* **2015**, *5*, 13801.
[36] K. J. P. Schouten, M. J. T. C. van der Niet, M. T. M. Koper, *Phys. Chem. Chem. Phys.* **2010**, *12*, 15217 – 15224.
[37] I. Ledezma-Yanez, W. D. Z. Wallace, P. Sebastián-Pascual, V. Climent, J. M. Feliu, M. T. M. Koper, *Nat. Energy* **2017**, *2*, 17031.
[38] K. Koh, U. Sanyal, M.-S. Lee, G. Cheng, M. Song, V.-A. Glezakou, Y. Liu, D. Li, R. Rousseau, O. Y. Gutiérrez, A. Karkamkar, M. Derewinski, J. Lercher, *Angew. Chem. Int. Ed.* **2020**, *59*, 1501 – 1505; *Angew. Chem.* **2020**, *132*, 1517 – 1521.
[39] D. C. Cantu, A. B. Padmaperuma, M.-T. Nguyen, S. A. Akhade, Y. Yoon, Y.-G. Wang, M.-S. Lee, V.-A. Glezakou, R. Rousseau, M. A. Lilga, *ACS Catal.* **2018**, *8*, 7645 – 7658.
[40] M.-T. Nguyen, S. A. Akhade, D. C. Cantu, M.-S. Lee, V.-A. Glezakou, R. Rousseau, *Catal. Today* **2020**, *350*, 39 – 46.
[41] N. Singh, U. Sanyal, G. Ruehl, K. A. Stoerzinger, O. Y. Gutiérrez, D. M. Camaioni, J. L. Fulton, J. A. Lercher, C. T. Campbell, *J. Catal.* **2020**, *382*, 372 – 384.
[42] Y. Yoon, R. Rousseau, R. S. Weber, D. Mei, J. A. Lercher, *J. Am. Chem. Soc.* **2014**, *136*, 10287 – 10298.
[43] N. Singh, M.-T. Nguyen, D. C. Cantu, B. L. Mehdi, N. D. Browning, J. L. Fulton, J. Zheng, M. Balasubramanian, O. Y. Gutiérrez, V.-A. Glezakou, R. Rousseau, N. Govind, D. M. Camaioni, C. T. Campbell, J. A. Lercher, *J. Catal.* **2018**, *368*, 8 – 19.
[44] S. J. Jenkins, *Proc. R. Soc. London Ser. A* **2009**, *465*, 2949 – 2976.
[45] M. L. Honkela, J. Bjork, M. Persson, *Phys. Chem. Chem. Phys.* **2012**, *14*, 5849 – 5854.
[46] M.-H. Ho, R. Rousseau, J. A. S. Roberts, E. S. Wiedner, M. Dupuis, D. L. DuBois, R. M. Bullock, S. Raugei, *ACS Catal.* **2015**, *5*, 5436 – 5452.
[47] S. Hammes-Schiffer, *J. Am. Chem. Soc.* **2015**, *137*, 8860 – 8871.
[48] G. Li, B. Wang, D. E. Resasco, *ACS Catal.* **2020**, *10*, 1294 – 1309.
[49] P. Sykes, *A guidebook to mechanism in organic chemistry*, 6th ed, 1996 pp. 61 – 63.
[50] J. Han, F.-M. Tao, *J. Phys. Chem. A* **2006**, *110*, 257 – 263.

[51] J. A. Lopez-Ruiz, E. Andrews, S. A. Akhade, M.-S. Lee, K. Koh, U. Sanyal, S. F. Yuk, A. J. Karkamkar, M. A. Derewinski, J. Holladay, V.-A. Glezakou, R. Rousseau, O. Y. Gutiérrez, J. D. Holladay, *ACS Catal.* **2019**, *9*, 9964 – 9972.
[52] R. Cretu, A. Kellenberger, M. Medeleamu, N. Vaszilcsin, *Int. J. Electrochem.* **2014**, *9*, 4465 – 4477.
[53] J. K. Nørskov, T. Bligaard, A. Logadottir, J. R. Kitchin, J. G. Chen, S. Pandelov, U. Stimming, *J. Electrochem. Soc.* **2005**, *152*, J23 – J26.
[54] J. Durst, C. Simon, F. Hasche, H. A. Gasteiger, *J. Electrochem. Soc.* **2015**, *162*, F190 – F203.
[55] J. Durst, A. Siebel, C. Simon, F. Hasché, J. Herranz, H. A. Gasteiger, *Energy Environ. Sci.* **2014**, *7*, 2255 – 2260.

Manuscript received: June 8, 2020
Revised manuscript received: July 27, 2020
Accepted manuscript online: August 7, 2020
Version of record online: October 27, 2020

